Continuous Topology Simplification of Planar Vector Fields

Xavier Tricoche[1] Gerik Scheuermann[1] Hans Hagen[1]

Abstract

Vector fields can present complex structural behavior, especially in turbulent computational fluid dynamics. The topological analysis of these datasets reduces the information but one is usually still left with too many details for interpretation. In this paper, we present a simplification approach that removes pairs of critical points from the dataset, based on relevance measures. In contrast to earlier methods, no grid changes are necessary since the whole method uses small local changes of the vector values defining the vector field. An interpretation in terms of bifurcations underlines the continuous, natural flavor of the algorithm.

Keywords: vector field topology, flow visualization, unstructured grid, simplification

1 Introduction

Topological methods are well-known techniques for the visualization of planar vector fields [1, 2]. They provide analysts with synthetic graph representations of vector data. This is achieved by the extraction of special features of a vector field called critical points and the integration of particular streamlines linking them in the corresponding flow known as separatrices: The resulting graph is a very reliable structural depiction. The theoretical framework is given by the qualitative theory of dynamical systems initiated by Poincaré [3] and continued by Andronov et al [4]. The success of this approach is due to its ability to offer automatic and intuitive depictions of large numerical data while dramatically reducing the amount of information required for interpretation.

Nevertheless, when dealing with turbulent flows provided by Computational Fluid Dynamics simulations (CFD) or experimental measurements of fluid mechanics, topology-based methods typically produce cluttered pictures that are of little help for physicists or engineers. Indeed, the topology of such flows is characterized by the presence of a large number of features of very small scale that greatly complicate the global depiction of the data. This problem explains the need for a simplification method that prunes insignificant features according to qualitative and quantitative criteria, specific to the considered application. Therefore, several techniques have been introduced in the visualization community that are concerned with vector field simplification. Nielson et al. have proposed a multi-resolution approach for planar vector fields defined over curvilinear grids [5]. Simplification is achieved by removing higher order details. Yet, topology is not the focus of this technique. The issue of topology simplification has been first addressed by de Leeuw et al. [6]. Their method removes pairs of critical points connected by the topological graph together with the corresponding edge while preserving consistency with the original topology. The method ignores the underlying continuous data. Consequently, no description of the vector field can be provided that corresponds to the simplified topology. The major drawback induced by this deficiency is that other classical flow visualization methods, e.g. streamlines or LIC [7], cannot be applied afterward to offer consistent depictions. In previous work [8], we proposed an alternative approach that merges close critical points, resulting in a higher order singularity that synthesizes the structural impact of several features of small scale in the large. This reduces the number of critical points as well as the global complexity of the graph. Nevertheless, this simplification can lead to the disappearance of meaningful features of the flow since only spatial criteria are taken into account. Furthermore, this approach is not able to remove critical points due to numerical noise.

The present method has been designed to overcome these drawbacks as well as to offer a continuous way to simplify the visualized topology. The basic principle, similar to the one used by de Leeuw, consists in successively removing pairs of connected critical points while preserving the consistency of the field structure. Each of these removals can be interpreted as a forced local deformation that brings a part of the topology to a simpler, equivalent structure. The mathematical background of such a deformation is given by the theory of bifurcations (see e.g. [9]). Practically, the method starts with a planar piecewise linear triangulation. We first compute the topological graph and associate every connection in the graph with numerical measures that evaluate its relevancy in the global structure. Next, we sort the corresponding pairs of critical points according to these criteria and retain those with values over prespecified thresholds. Then we process all pairs sequentially: for each of them, we first determine a cell pad enclosing both critical points. In this pad, we slightly modify the vector values such that both critical points disappear. This deformation is controlled by angular constraints on the new vector values imposed by those kept constant on the frame of the pad. When every pair has been processed, we draw the simplified topology.

The paper is structured as follows. We review basic notions of vector field topology and briefly present the notion of bifurcation in section 2. In section 3, we show how we compute the topology in a way suited for further processing. Numerical measures used to evaluate the relevancy of critical points and separatrices are introduced in section 4: This provides pairs of critical points to be removed. The next section details how local deformations of the vector field are conducted to suppress the selected pairs. Results are proposed on a CFD dataset in section 6.

2 Vector Field Topology

In the present method, we deal with a triangulation of vertices lying in the plane associated with 2D vector values. The interpolation scheme is piecewise linear. Therefore, we only consider topological features of first order. In this case, topology is defined as the graph built up of all first-order critical points, closed orbits and some particular integral curves connecting them, called separatrices. We review these notations.

[1]Computer Science Department, University of Kaiserlautern, P.O. Box 3049, D-67653 Kaiserslautern, Germany,
{tricoche,scheuer,hagen}@informatik.uni-kl.de

2.1 Critical Points

The *critical points* (or singular points) of a vector field are the positions where the field magnitude is zero. These points play a fundamental role in the field structure because they are the only locations where streamlines can meet. The classification of critical points is based, in the linear case, upon the eigenvalues of the Jacobian matrix of the field at their position. Depending on the real and imaginary parts of these eigenvalues, there exist several basic configurations, as shown in Fig. 1. Of particular interest are the *saddle points* because the *separatrices* start or end at their location along the eigenvectors. Note that for every other critical point type, the sign of the real parts of the eigenvalues is either positive or negative, corresponding to a repelling (source) or an attracting (sink) nature, respectively. Thus separatrices emanate from saddle points and end at sources or sinks. The *basin* of a source (resp. sink) is defined as the set of all points lying on streamlines coming from (resp. tending to) it.

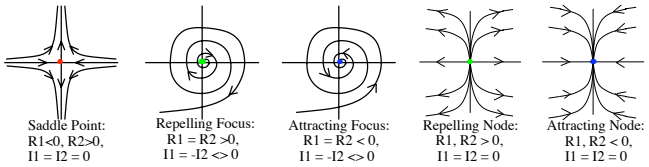

Figure 1: Basic configurations of 1st-order critical points

2.2 Closed Orbits

Some topological features play the role of a source or sink in a vector field and are not reduced to single points: These are closed orbits, also called limit cycles because of the asymptotic behavior of the streamlines in their vicinity. Fig. 2 illustrates such a configuration. These cycles are actually periodic streamlines.

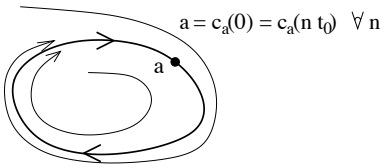

Figure 2: Attracting closed orbit (sink)

2.3 Poincaré Index

A fundamental concept in vector field topology is the so-called Poincaré index of a simple closed curve: It measures the number of rotations of the vector field while traveling along the curve in positive direction. In a more mathematical way, one gets the following definition for the index of a simple curve γ:

$$\text{index}_\gamma = \frac{1}{2\pi} \oint_\gamma \mathrm{d}\phi, \quad \text{where} \quad \phi = \arctan\frac{v_y}{v_x}.$$

(ϕ is the angle coordinate of the vector field $\vec{v}(v_x, v_y)$.) Remind that the index is always an integer. One can extend this definition and introduce the index of a critical point: This is the index of a simple closed curve around the critical point enclosing no other singular point. For first order critical points (see section 2.1), the possible index values are +1 and -1: A saddle point has index -1 whereas every other critical point has index +1. Note that the index of a closed orbit is always +1. We give now two fundamental theorems related to the notion of index, see Andronov et al. [4] for a rigorous presentation.

Theorem 2.1 *A simple closed curve that encloses no critical point has index 0.*

Theorem 2.2 *The index of a simple closed curve that encloses several critical points is the sum of the respective indices of those critical points.*

In our case, the critical points that may be encountered in the interior domain of each linearly interpolated triangle cell are of first order and have therefore either index +1 or -1. Consequently, considering the edges of a triangle as simple closed curve in theorem 2.1, and using the fact that at most one singular point can be found in a linear vector field, we get the following property.

Property 2.1 *There is no singular point in a triangle cell* if and only if *this cell has index 0.*

Furthermore, the linear interpolation greatly simplifies the practical computation of the index of a triangle cell. As a matter of fact, the angle coordinate change along a linearly interpolated edge is always smaller than π, as shown in Fig. 3. Consequently, the index

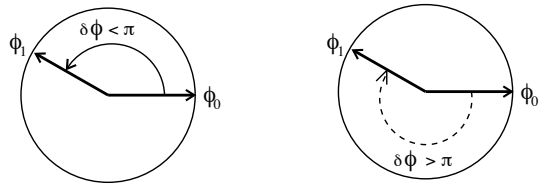

Figure 3: Angular rotation along a linear edge

of a triangle cell is given by the sum of the angle changes: Let ϕ_0, ϕ_1 and ϕ_2 be the angle coordinates ($\in [0, 2\pi[$) of the vectors $\vec{v}_0$, $\vec{v}_1$ and $\vec{v}_2$ defined at the vertices of a linearly interpolated triangle. The index of this triangle T is given by

$$\text{index}(T) \quad = \quad \frac{1}{2\pi}\left(\Delta(\phi_0, \phi_1) + \Delta(\phi_1, \phi_2) + \Delta(\phi_2, \phi_0)\right) \quad (1)$$

$$\text{where} \quad \Delta(\phi_i, \phi_j) = \begin{cases} \phi_j - \phi_i + 2\pi & \text{if } \phi_j - \phi_i < -\pi, \\ \phi_j - \phi_i & \text{if } |\phi_j - \phi_i| < \pi, \\ \phi_j - \phi_i - 2\pi & \text{if } \phi_j - \phi_i > +\pi, \end{cases}$$

Remark: Vector magnitudes have no influence on the triangle index and therefore on the presence of a singularity inside the cell.

2.4 Parameter Dependent Topology

The mathematical concept behind our approach of topology simplification is the notion of parameter dependent topology. Indeed, the definitions introduced previously deal with an instantaneous topological state of a vector field. Now, as we know from the theory of dynamical systems, this stable state may evolve in another one by slight changes of underlying parameters of the field. This is intuitively clear when considering time-dependent vector fields: The topology changes over time by the move, appearance or vanishing

of critical points. These changes always respect qualitative consistency. In particular, the poincaré index acts as topological invariant which explains its fundamental importance. Local qualitative modifications in the field structure that respect this consistency are known as *local bifurcations*. In the case of linear parameter changes we are concerned with, one mostly encounters two kinds of local bifurcations. The first one consists in the pairwise annihilation of two critical points of opposite indices (in our case a saddle point and a sink or source). Since these singularities have global index 0 (in the sense of theorem 2.2), they are equivalent to a configuration without critical point and therefore disappear right after merging. An illustration of this phenomenon is proposed in section 5.4. The reverse transformation is also possible: This is a pairwise creation. The second kind of common local bifurcation is the so-called Hopf bifurcation: A critical point of index +1, say a sink, becomes a source (both have index +1). Global consistency of the flow is preserved by the simultaneous creation of a sink closed orbit surrounding the source. Once again, the reverse case may occur too: A source becomes a sink with disappearance of a surrounding source closed orbit. This bifurcation is illustrated in Fig. 4.

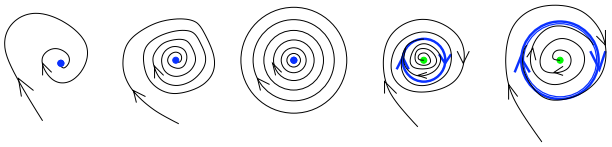

Figure 4: Hopf bifurcation

Practically, since we want to reduce the number of critical points while being consistent with the original topology, we locally force pairwise annihilations of a saddle point and a sink or source. This can be done by small local changes in the field values as we show in the following. An illustration of this mathematical interpretation of topology simplification is proposed in section 5.4.

3 Topology Computation

As a preprocessing step, our method requires the computation of the topological graph. This computation must be conducted in a way that provides all the information needed for pairing critical points as explained in the next section.
Consequently, we process as follows: We start with the computation of all critical points in the grid. From each saddle point, we integrate the four related separatrices. For each separatrix, we check if it leaves the grid or if it reaches a critical point or a closed orbit. An accurate and effective detection of closed orbits is achieved thanks to a scheme described elsewhere [10]. If a critical point is reached (sink or source, depending on the integration direction from the saddle point), we identify it among the set of all critical points and save this information for the current separatrix. Furthermore, we mark this sink or source as `connected`. If a closed orbit is reached, we must await the end of the complete topology computation to process this separatrix further. As a matter of fact, once all separatrices have been integrated, we look over all singularities for sinks or sources that are not `connected` and associate them with the separatrix surrounding the cycle that contains them, if any. This supposes that a single critical point (with index +1, c.f. index of a closed orbit) is present inside each limit cycle. Actually, any topological structure of index +1 may be encountered inside a closed orbit even if a single sink or source is most likely to occur. At last, the separatrix gets as length the Euclidean distance between saddle point and isolated critical point. The reason for this choice is explained in the next section. Possible cases are illustrated in Fig. 5. This completes the topological information required for further processing.

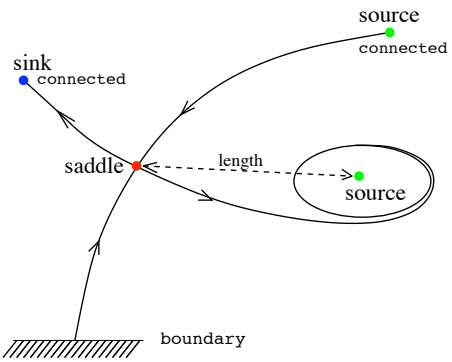

Figure 5: Topological connections of a saddle point

4 Pairing Strategy

The basic idea behind our simplification technique is to use the topological equivalence (in the sense of the index invariant) of a region containing several critical points with index sum 0 (see theorem 2.2) with the same region without critical point. More precisely, we aim at removing pairs of first order critical points of opposite index (that is a saddle point - index -1 - and a source or sink - index +1 -) to reduce the number of singularities present in the field and thus simplify the resulting topology while keeping consistent with the original structure. To achieve it, we first need to determine which pairs of critical points may be removed in that way and to classify them according to the significance of the singularities in the field structure.

4.1 Connectivity

We require the singular points of a pair to be linked by a separatrix in the topological graph. This ensures that the topological transition associated with the disappearance of both singularities corresponds to a local bifurcation (see section 2.4). Yet, this criterion must be relaxed to handle isolated singularities lying in the interior domain of a closed orbit. This explains why we decided previously to connect a saddle point with an isolated critical point across the limit cycles enclosing it.

4.2 Additional Criteria

The importance of critical points mainly depends on the interpretation of the visualized vector field. For this reason, one can make use of different measures to classify the relevance of critical points and possibly consider a weighted combination of several of them to fit the domain of application.
Relevancy measures are for instance the Euclidean distance between critical points, or the length of the edge (separatrix) connecting them (both measures apply to a pair of critical points of opposite indices), or the degree of a critical point of index +1 (sink or source), that is the number of saddle points it is connected to. Furthermore, in [6], the authors suggest to use the area of a source or sink's basin (see section 2.1) to evaluate the importance of critical points of index +1. Yet this basin-based method implies a computational effort that makes it unsuited for our method. Another interesting quantity based upon fluid dynamics considerations is the

absolute value of the vorticity of a sink or source. Spatial variation of vorticity in the vicinity of a critical point of index +1 also gives insight into the action of a source or sink on the field structure. Nevertheless, an accurate computation of such quantities is a tricky task, especially in the quite common case of planar vector fields cut off from 3D datasets: Higher order terms are involved and, when dealing with simulations, the underlying numerical schemes must be taken into account, and not only the given discrete values. Eventually, a simple numerical measure we are concerned with in the present method is the maximal magnitude of the vector field in a cell containing a critical point of index +1. This permits to remove singularities that are due to numerical noise and inconvenience interpretation.
Practically, we have adopted two complementary criteria: On one hand we apply a threshold on the Euclidean distance of both points of a pair and preserve the pairs with largest lengths. On the other hand, we choose to maintain every source or sink lying in a cell with minimum magnitude over a second threshold.

With this definition, critical points belonging to several valid pairs will be simplified concurrently: We process the pairs in increasing length's order and skip those that contain singularities that have been removed already.

5 Local Deformation

Once a pair of critical points has been identified that fulfills our criteria, it must be removed. To do this, we start a local deformation of the vector field in a small area around the considered singular points. To preserve both the interpolation scheme and the grid structure, we only modify vector values at grid vertices. In the following, we detail how we determine which vertices have to get a new vector value and how we set the new values in order to ensure the absence of a singularity in the concerned cells after processing. At last, we illustrate the continuity of this deformation.

5.1 Cell-wise Connection

Consider the situation shown in Fig. 6. We first compute the intersections of the straight line connecting the first critical point to the second with the edges of the triangulation. For each intersection point, we insert the grid vertex closest to the second critical point (see vertices surrounded by a circle) in a temporary list . After this, we compute the bounding box of all vertices in the list and include all grid vertices contained in this box. This obviously includes every vertex marked in the former step. The use of a bounding box

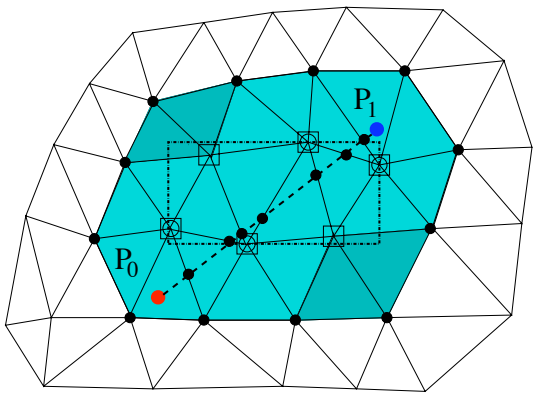

Figure 6: Cell-wise connection

is intended to ensure a well shaped deformation domain, especially useful if many cells separate both singular points. This configuration occurs if the threshold has been assigned a large value to obtain a high simplification rate. The vertices concerned with modification are surrounded by squares. We call them *internal vertices* in the following. Since the modification of a vertex vector value has an incidence on the indices of all triangle cells it belongs to, we include every cell incident to one of the selected vertices in a cell group. These cells are colored in gray. Further processing will have to associate the internal vertices with vector values that ensure the absence of any singular point in the cell group with respect to the vector values defined at the *boundary vertices* (marked by big dots in Fig. 6) that will not be changed. Note that the connection may fail if one of the included cells contains a critical point that does not belong to the current pair: In this case, the global index of the cell group is no longer zero. If it occurs, we interrupt the processing of this pair. Nevertheless, such cases can be mostly avoided by simplifying pairs of increasing distance.

5.2 Angular Constraints

To give insight into our deformation strategy, we first consider a single internal vertex and its incident cells as shown in Fig. 7. Suppose that every position marked in black is associated with a constant vector value and that the corresponding global index of all triangles (in the sense of theorem 2.2) is zero. The problem then consists in determining a new vector value at the internal vertex (in white) such that no incident cell contains a critical point. According to property 2.1, this is equivalent to the fact that every incident triangle has index 0. Now, in each triangle, the angle coordinates

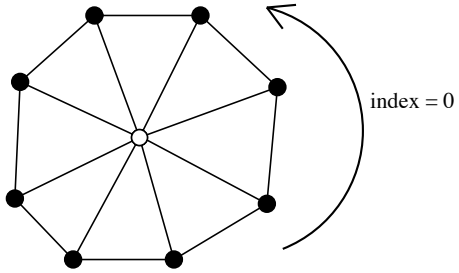

Figure 7: Configuration with single intern vertex and incident cells

of the vectors defined at the black vertices induce an angular constraint for the new vector (We saw in section 2.3 that the index in a cell does not depend on the magnitude of the vectors defined at its vertices.) As a matter of fact, in equation 1, $\Delta(\phi_0, \phi_1)$ is already set to a value that is strictly smaller than π. The two missing terms must induce a global angle change smaller than 2π (for an index is an integer). It will be the case if and only if the new vector value has angle coordinate in $]\phi_1 + \pi, \phi_0 + \pi[$, with $[\phi_0, \phi_1]$ being an interval with width smaller than π, i.e. the angle change along a linear edge occurs from ϕ_0 to ϕ_1 (see Fig. 8). This provides a constraint on the new value for a single triangle. Intersecting the intervals induced by all incident triangles, one is eventually able to determine an interval that fulfills all the constraints. Note that this interval may be empty. In this case, the simplification is (at least temporarily) impossible. As far as the magnitude of the new vector is concerned, one simply takes the mean value of the field magnitude on the exterior edges. Once again, the linear interpolant defined on these edges facilitates the computation of this quantity.

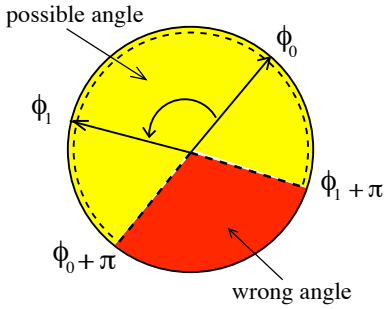

Figure 8: Angular constraint in a triangle cell

5.3 Iterative Solution

When considering all internal vertices as shown in Fig. 6, one must find, for each of them, a new vector value that fulfills all the constraints induced by the edges connecting their incident vertices. These incident vertices are of two types: internal or boundary vertices. Edges linking boundary vertices are considered constant and induce therefore fixed constraints. Internal vertices on the contrary, still must be provided a final vector value and introduce consequently flexibility in the simplification scheme (see Fig. 9).

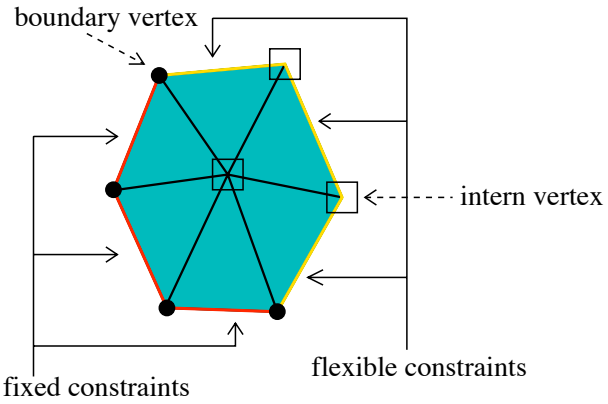

Figure 9: Different types of constraints for an intern vertex

Our method is then as follows.

```
// initialisation
for_each (intern vertex)
   interval = fixed constraints
   if (interval is empty)
      interrupt
   endif
   if (no fixed constraints)
      interval = [0,2PI[
   end if
end for_each

// iterations
nb_iterations = 0
repeat
   succeeded = true
   nb_iterations++
   for_each intern vertex
      compute mean vector of defined
         incident vertices
      if (interval is not empty)
         if (mean vector in interval)
            current_value = mean vector
         else
            current_value =
               best approximation of
               mean vector in interval
         end if
      else
         succeeded = false
         if (mean vector in fixed
             constraints)
            current_value = mean vector
         else
            current_value =
               best approximation of
               mean vector in interval
      end if
   end for_each
until (succeeded or
       nb_iterations > MAX_NB_ITERATIONS)
```

If one of the internal vertices has incompatible fixed constraints, our scheme cannot succeed. Therefore we interrupt the process during initialization and move to the next pair. If the iterative process failed at determining compatible angular constraints for every internal vertices, we maintain the current pair and move to the next as well.

5.4 A Continuous Deformation

As said previously, each local deformation of the vector field associated with the removal of a pair corresponds to a pairwise annihilation of two critical points of opposite index. The continuity of this transition can be illustrated by linearly interpolating, for each modified vertex, its value between the original vector value and the one obtained after modification. Depicting each intermediate aspect of the topology in the vicinity of both critical points shows how they become closer to merge and finally disappear. Considering time as third dimension, one gets the picture proposed in Fig. 10.

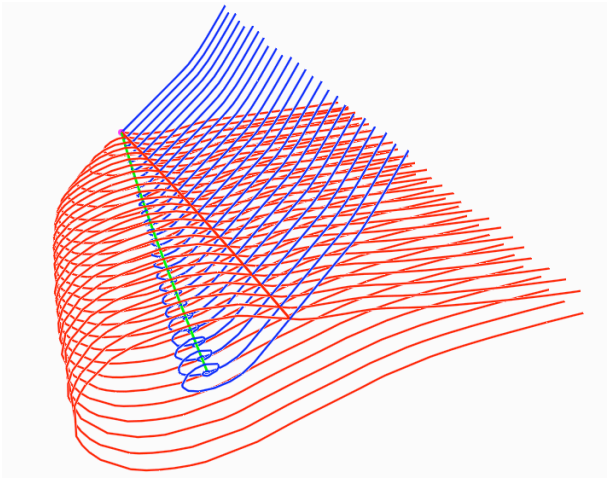

Figure 10: Continuous topological transition

6 Results

We show next the results of our method applied to a vortex breakdown simulation. More precisely, we deal with a swirling jet simulation: This type of flow is important to combustion applications where they are able to create recirculation zones with sufficient residence time for the reactions to approach completion. The grid is rectilinear and has 124 x 101 vertices ranging from 0 to 9.84 in x and from -3.864 to 3.864 in y. The triangulation has 24600 linearly interpolated cells. The original topology is shown in Fig. 11 together with the underlying grid structure. (Fig. 17 offers a depiction of the topology over a LIC representation.) There are 94 critical points and 134 corresponding pairs. We first simplify without

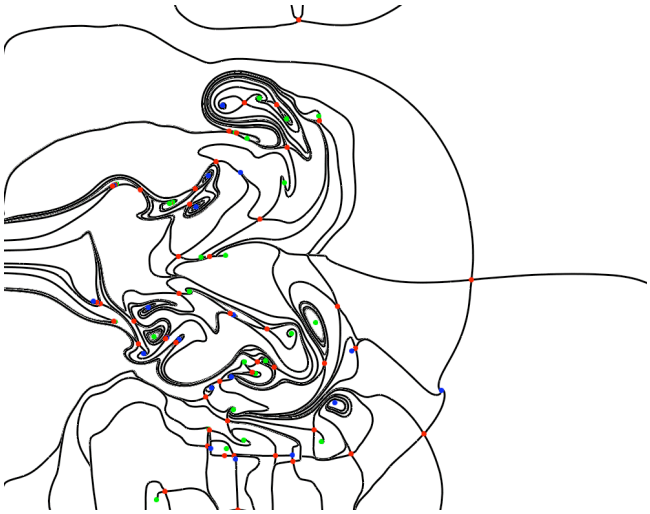

Figure 11: Original topology

magnitude control. The only threshold is therefore the graphical distance between critical points. We apply increasing thresholds ranging from 1% to 50% of the grid width to select the pairs to simplify. The table proposed next puts the corresponding results together.

threshold	satisfying pairs	connected pairs	removed pairs	removed sing.
1%	13 (10%)	10 (7%)	10 (7%)	20 (21%)
5%	24 (18%)	19 (14%)	19 (14%)	38 (40%)
10%	40 (30%)	27 (20%)	27 (20%)	54 (57%)
20%	65 (49%)	36 (27%)	34 (25%)	68 (72%)
50%	90 (67%)	40 (43%)	38 (40%)	76 (81%)

The pictures associated with the thresholds 5% and 50% are shown in Fig. 12 and Fig. 13 respectively. The first topology contains 56 critical points whereas there are only 18 singularities remaining in the second one. If we focus on a small part of the topology, we observe how features of small scale are removed: Compare Fig. 14 and Fig. 15.

If we choose, on the contrary, to restrict the simplification to a filtering of computational noise by the use of a threshold on the field magnitude, we get the results presented in the following table (the threshold is expressed with respect to the largest norm of the vector field).

threshold	satisfying pairs	connected pairs	removed pairs	removed sing.
0.5%	25 (19%)	8 (6%)	8 (6%)	16 (17%)
1%	30 (22%)	11 (8%)	11 (8%)	22 (23%)
5%	47 (35%)	15 (11%)	15 (11%)	30 (32%)
10%	77 (57%)	21 (16%)	21 (16%)	42 (45%)
20%	95 (71%)	28 (21%)	26 (19%)	52 (55%)
50%	115 (86%)	36 (27%)	33 (25%)	66 (70%)

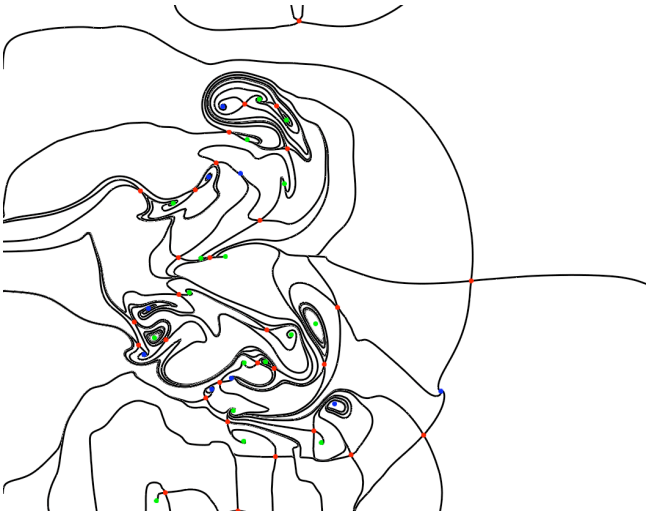

Figure 12: Simplified topology: Small graphic threshold (5%)

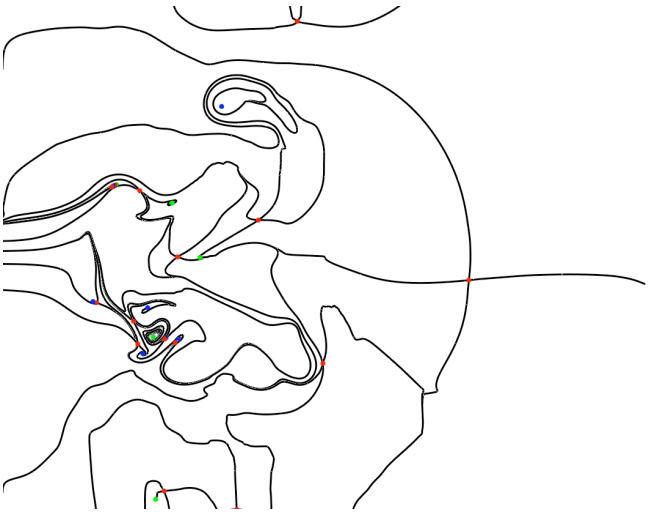

Figure 13: Simplified topology: Large graphic threshold (50%)

The picture shown in Fig. 16 illustrates the topology obtained after simplification with a very low threshold (0.5%) on the magnitude. The graph presents then 78 critical points.

At last, we propose in Fig. 18 the topology obtained when the simplification is applied without distance nor norm threshold. This obviously leads to the highest simplification rate that can be reached by our method for this particular dataset. The 14 critical points remaining correspond to configurations that can be resolved by the method. Nevertheless, in this depiction, no visual clutter is present and the original structural complexity has been greatly clarified.

7 Conclusions

We have presented a method that simplifies the topology of turbulent planar vector fields while respecting structural consistency with the original data. It is based upon successive local modifications of the vector field that permit the disappearance of pairs of critical points. These pairs are determined and sorted according to

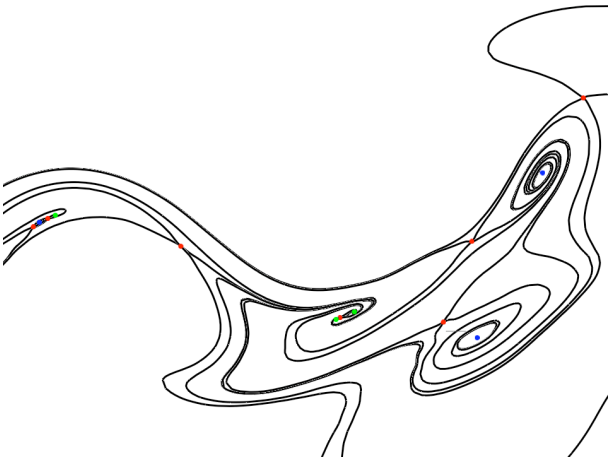

Figure 14: Close up of the original topology

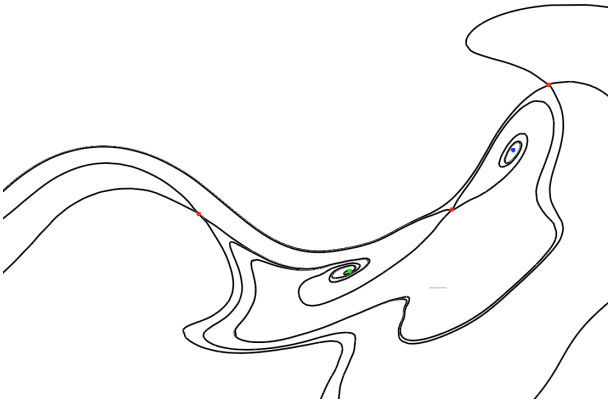

Figure 15: Close up of the simplified topology

graphical and numerical criteria that can be adapted to the domain of application. The whole method can be seen as a continuous process where local bifurcations are forced, that entail the merging and annihilation of critical points of opposite index. We have tested our algorithm on a numerical dataset provided by a CFD simulation. The results demonstrate the ability of the method to filter numerical noise on one hand and prune structural features of small scale on the other hand. This clarifies the depiction and eases interpretation.

Acknowledgment

The authors wish to thank Wolfgang Kollmann, MAE Department of UC Davis, for providing the swirling jet dataset. Furthermore, we would like to thank Tom Bobach and Jan Frey for their programming efforts.

References

[1] Helman J.L., Hesselink L., *Visualizing Vector Field Topology in Fluid Flows*. IEEE Computer Graphics and Applications, 1991. pp.36-46.

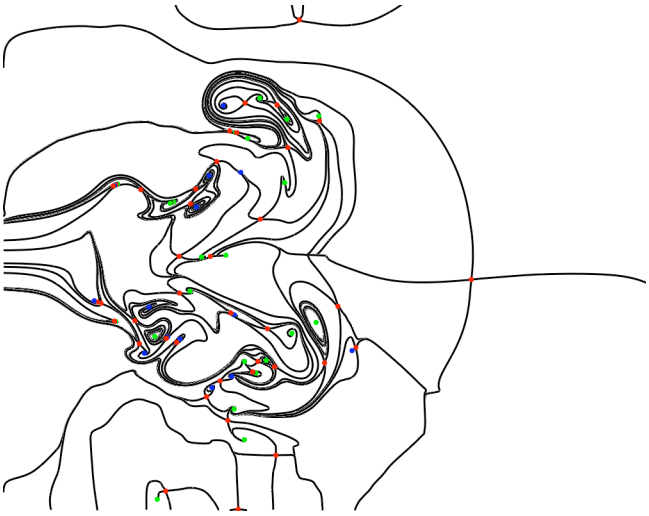

Figure 16: Simplified topology: Low noise filter (0.5% of maximal magnitude)

[2] Globus A., Levit C., Lasinski, T., *A Tool for Visualizing of Three-Dimensional Vector Fields*. In Proceedings of IEEE Visualization '91, IEEE Computer Society, San Diego, CA, 1991, pp. 33-40.

[3] Poincaré H., *Sur les courbes définies par une équation différentielle*. Oeuvres, Vol. I., Paris, Gauthier-Villars, 1928.

[4] Andronov A.A., Leontovich E.A., Gordon I.I., Maier A.G., *Qualitative Theory of Second-Order Dynamic Systems*. Israel Program For Scientific Translation, Halsted Press, 1973.

[5] Nielson G.M., Jung I.H., Song. J., *Wavelets over Curvilinear Grids*. In Proceedings of IEEE Visualization '98, IEEE Computer Society, Research Triangle Parck, NC, 1998, pp. 313-317.

[6] de Leeuw W., van Liere R., *Collapsing Flow Topology Using Area Metrics*. In Proceedings of IEEE Visualization 99, IEEE Computer Society, Los Alamitos, CA, 1999, pp. 349-354.

[7] Cabral B, Leedom L., *Imaging Vector Fields Using Line Integral Convolution*. In SIGGRAPH '93 Proceedings, ACM, New York, NY, 1993, pp. 263-270.

[8] X. Tricoche, G. Scheuermann, H. Hagen, *A Topology Simplification Method for 2D Vector Fields*. In Proceedings IEEE Visualization'00, IEEE Computer Society, Los Alamitos CA, 2000, pp.359-366.

[9] Guckenheimer J., Holmes P., *Nonlinear Oscillations, Dynamical Systems, and Bifucations of Vector Fields* Applied Mathematical Sciences 42, Springer-Verlag, 1983.

[10] Wischgoll T., Scheuermann G., *Detection and Visualization of Closed Streamlines in Planar Flows*. To appear in IEEE Transactions on Visualizations and Computer Graphics, IEEE Computer Society, Los Alamitos, CA, 2001.

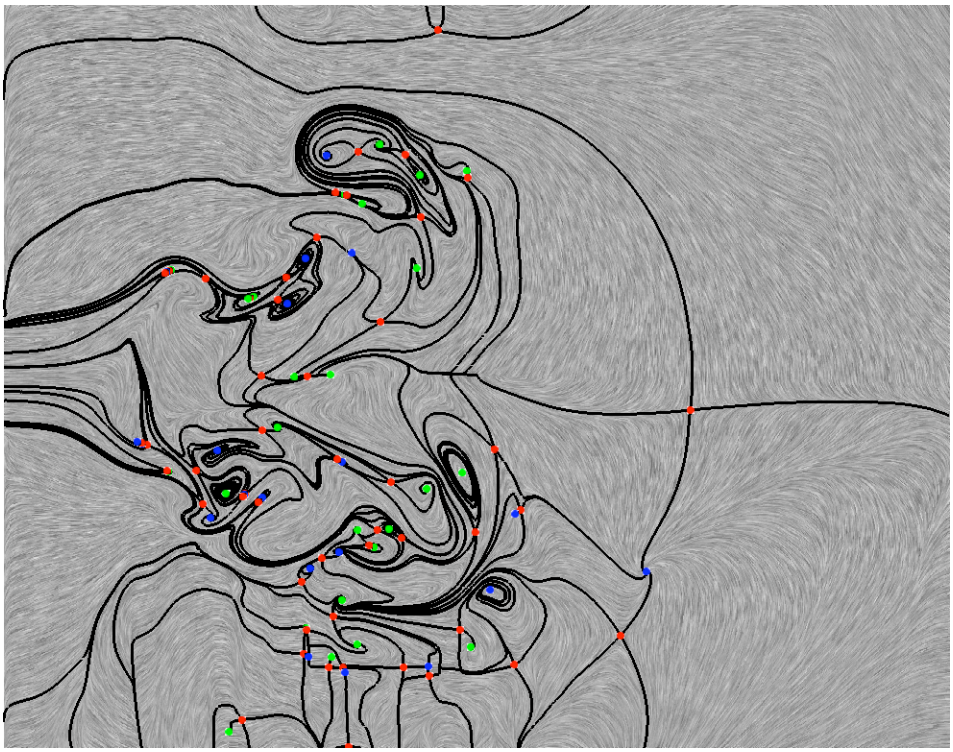

Figure 17: Original topology and LIC representation

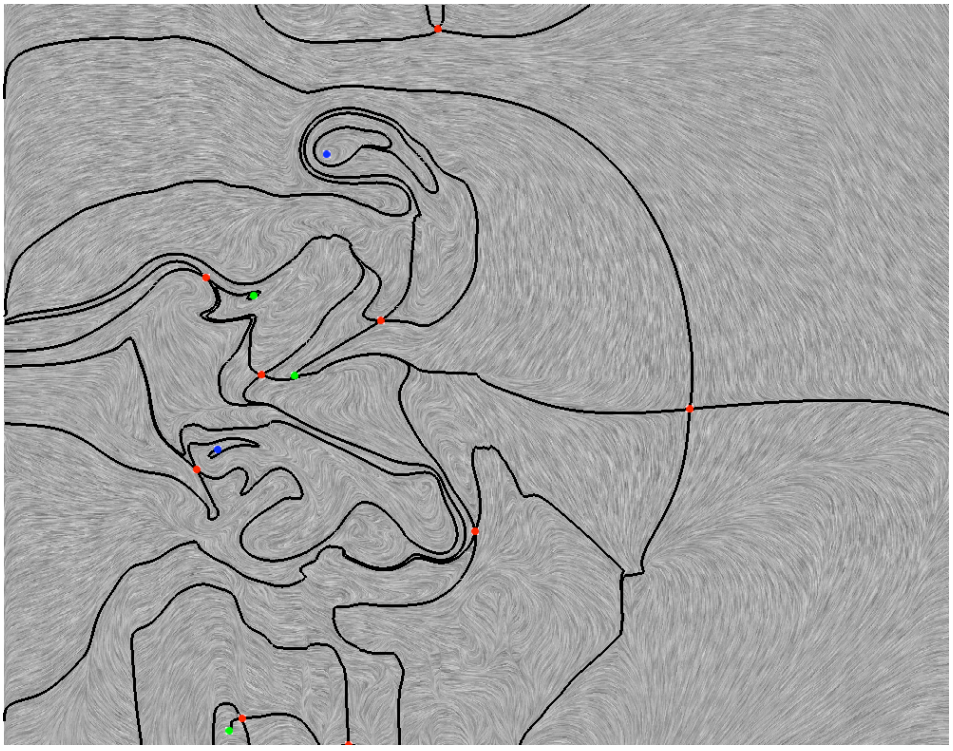

Figure 18: Simplified topology: Maximal simplification rate and LIC representation